Pacific Graphics 2010
P. Alliez, K. Bala, and K. Zhou
(Guest Editors)

Volume 29 (2010), Number 7

Condenser-Based Instant Reflectometry

Yanxiang Lan [†] [‡] Yue Dong[†] [‡] Jiaping Wang[‡] Xin Tong [‡] Baining Guo [‡] [†]

[†] Tsinghua University [‡] Microsoft Research Asia

Abstract

We present a technique for rapid capture of high quality bidirectional reflection distribution functions(BRDFs) of surface points. Our method represents the BRDF at each point by a generalized microfacet model with tabulated normal distribution function (NDF) and assumes that the BRDF is symmetrical. A compact and light-weight reflectometry apparatus is developed for capturing reflectance data from each surface point within one second. The device consists of a pair of condenser lenses, a video camera, and six LED light sources. During capture, the reflected rays from a surface point lit by a LED lighting are refracted by a condenser lenses and efficiently collected by the camera CCD. Taking advantage of BRDF symmetry, our reflectometry apparatus provides an efficient optical design to improve the measurement quality. We also propose a model fitting algorithm for reconstructing the generalized microfacet model from the sparse BRDF slices captured from a material surface point. Our new algorithm addresses the measurement errors and generates more accurate results than previous work.

Our technique provides a practical and efficient solution for BRDF acquisition, especially for materials with anisotropic reflectance. We test the accuracy of our approach by comparing our results with ground truth. We demonstrate the efficiency of our reflectometry by measuring materials with different degrees of specularity, values of Fresnel factor, and angular variation.

1. Introduction

Real world surfaces exhibit rich reflectance properties, such as anisotropic specularity and Fresnel effects. Capturing these reflectance properties from real world surfaces is a fundamental and challenging problem in computer graphics.

Surface reflectance at a single point can be described by the four dimensional *Bidirectional Reflectance Distribution Function* (BRDF) [NRH*77] $\rho(\mathbf{i},\mathbf{o})$ that represents the radiance reflected from direction $\mathbf{o}$ divided by the incident radiant flux density from direction $\mathbf{i}$. A number of systems have been developed to measure BRDF from real world surface [LKK98, MWL*99, Dan01, MPBM03b] by densely sampling the viewing and lighting directions. High resolution BRDF acquisition requires lengthy capture time or a complicated device setup. Several compact devices [HP03, Msy07, BEWB*08] have been proposed for fast BRDF acquisition. However, it still takes tens of minutes for capturing a high resolution BRDF from surface.

Another set of methods measure the radiance of a surface point under a sparse set of viewing and lighting conditions and reconstruct the parametric BRDF model from the sparse measurements [War92, LFTG97, LKG*03, GTHD03, LLSS03]. Although these methods greatly simplify the acquisition process, they fail to capture the detailed reflectance and anisotropic specularities of many real materials [NDM05, WZT*08].

Recently, we [DWT*10] presented a technique for fast BRDF acquisition, in which the BRDF is represented by a generalized microfacet model [APS00] with tabulated 2D normal distribution function (NDF). A condenser based handheld device is developed for densely sampling the rays reflected from a surface point lit by each LED light source. The generalized microfacet model is then reconstructed from the measured data with the method in [NDM05]. Although this method provides an efficient solution for fast BRDF acquisition, it still has several limitations. First, with sparse LED light sources, the method only captures reflectance details determined by central region of the NDF and thus fails to measure the detailed reflectance resulting from other regions of the NDF. Moreover, partial rays reflected from the surface are occluded by one LED light source and thus the result resolution is decreased. Second, the algorithm used

to estimate the Fresnel factor is sensitive to the noise in the captured data. Finally, the reconstruction algorithm is fragile and cannot well handle the errors generated by the capturing process.

In this paper, we propose a new condenser-based instant reflectometer for fast BRDF acquisition, which greatly improves the accuracy and robustness of the method in [DWT*10]. Our method also models the BRDF at each point with the generalized microfacet model with tabulated NDF. The key observation of our method is that many BRDFs of physical materials are symmetrical across their surface normals [HLHZ08]. With this in mind, we present a new condenser based apparatus with optimized optical design, which provides more NDF coverage and avoids the occlusions caused by LED light sources as in [DWT*10]. A new reconstruction algorithm is proposed to estimate the Fresnel factor and the NDF iteratively, which improves the fitting accuracy and robustness. Moreover, our reconstruction algorithm can well handle the errors introduced by capturing process. For BRDFs that are not symmetrical across their normals, an adapted microfacet synthesis algorithm [WZT*08] is applied for reconstructing BRDFs from the captured data.

Compared to the technique presented in [DWT*10], our new reflectometry not only keeps the compact design and fast acquisition speed, but also provides an accurate and robust solution for BRDF acquisition, especially for materials with anisotropic reflectance. We test our approach by comparing our results with ground truth and demonstrate the efficiency of our reflectometry with a set of BRDFs measured from real materials, including 18 isotropic BRDFs and 12 that are anisotropic.

2. Related Works

2.1. Brute Force BRDF Sampling

A set of gonioreflectometers have been developed for capturing BRDFs [MPBM03b], SVBRDFs(spatially varying BRDFs) [DNvGK99, MLH02, LBAD*06, GTR*06], BTFs (bidirectional texture functions) [Dan01, MMS*05] and reflectance fields [GTLL06]. To densely sample the viewing and lighting directions, these devices either need specialized rigs for moving two of three components (light source, camera and material sample), or a dome with multiple cameras and lights. Although several techniques have been proposed to reduce the samples by exploiting BRDF properties [LLSS03], and spatial distribution [MWL*99, LKK98], the acquisition process still takes long time or requires expensive device setup.

Han et al. [HP03] developed a kaleidoscope-based apparatus for fast BTF measurement. The device is not capable of high quality BRDF measurement due to the limited angular resolution. Moshe et al. [BEWB*08] presented a compact BRDF capturing device that uses LEDs for both light emitters and receivers. Although this technique can quickly capture the BRDF, the sampling resolution is low. Mukaigawa et. al. [Msy07] proposed an ellipsoidal mirror based device for fast BRDF measurement. Although this device can capture dense BRDF samples, it takes ten of minutes to acquire a high resolution BRDF. Our BRDF capturing device is based on condenser lens and allows us to quickly capturing the reflectance of a point over the surface.

2.2. Fitting Reflectance Model

Several methods [War92, LFTG97, GTHD03, LKG*03, KN06] represent BRDFs with a parametric model and fit it with sparse measurements. Although these methods work well for material with simple reflectance, they cannot accurately capture reflectance details and anisotropic specularities [NDM05].

Romeiro et al. [RVZ08] represented the isotropic BRDF with a bi-variate model and reconstructed the BRDF from set of images of material sphere taken under passive lighting. However, this method cannot be used to capture the BRDF from a textured surface. Also, it is not clear how to extend this method for capturing the anisotropic BRDF of real materials.

The generalized microfacet model [APS00] represents the rich details of a BRDF with a 2D tabulated normal distribution function, which can be efficiently reconstructed from a set of 2D BRDF slices. Debevec et al. [DHT*00] captured the reflectance of human face under all lighting directions from a single view and reconstructed the generalized microfacet model at each point with fixed Fresnel factors. In [WZT*08], the partial NDF at each point is reconstructed from reflectance data measured from single view and dense lighting. The full NDF at each point is then completed via synthesis. Both methods use special device for lighting and take a long time for capture. In our method, we capture dense rays reflected from surface point under sparse lighting. By warping the reflected rays into camera CCD, our method can capture the reflectance data of each surface point within seconds.

3. Design Principles

Our reflectometry apparatus is designed for the general microfacet BRDF model. The microfacet BRDF model reduces the 4D BRDF into a 2D normal distribution function, and enables fast acquisition, On the other hand, this model is general enough and capable to accurately reproduce the physical reflectance properties. By introducing the microfacet BRDF model, our method only requires $n_l = 6$ lighting conditions to reconstruct a high quality general microfacet BRDF, while capturing a raw BRDF data often requires much denser light sampling.

In addition, symmetry is a common property exhibits in real-world BRDFs. Taking advantages of the BRDF symmetry property, we can further reduce the required sampling density while preserving the quality of results.

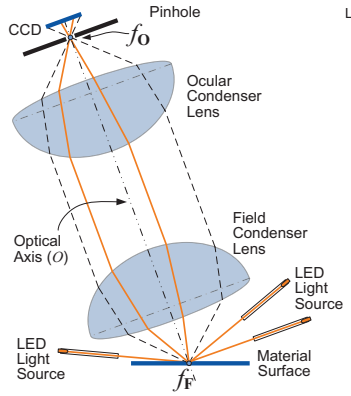

LED and Condenser Positions

	θ	ϕ
O	20°	0°
l_1	85°	0°
l_2	75°	60°
l_3	80°	180°
l_4	65°	240°
l_5	75°	300°
l_6	45°	170°

Figure 1: *The optical design of the condenser-based reflectometer is shown on the left. The positions of the condenser optical axis and LED light sources are listed on the top right. The bottom right shows a photo of the prototype reflectometer.*

3.1. The Microfacet BRDF Model

Based on microfacet theory, the reflectance of a surface point from the lighting direction $\mathbf{i}$ to the viewing direction $\mathbf{o}$ can be decomposed into the diffuse and specular components with a diffuse efficient k_d and a specular coefficient k_s:

$$\rho(\mathbf{i},\mathbf{o}) = k_d/\pi + k_s\rho_s(\mathbf{i},\mathbf{o}) \tag{1}$$

The specular term then can be represented by a general microfacet model:

$$\rho_s(\mathbf{i},\mathbf{o}) = \frac{D(\mathbf{h})\,S(\mathbf{i})\,S(\mathbf{o})\,F(\mathbf{o},\mathbf{i})}{4\,(\mathbf{i}\cdot\mathbf{n})\,(\mathbf{o}\cdot\mathbf{n})}, \tag{2}$$

Where $\mathbf{h} = (\mathbf{o}+\mathbf{i})/|(\mathbf{o}+\mathbf{i})|$ stands for the half-vector, and $\mathbf{n}$ is the surface normal.

The reflectance appearance is dominated by the *normal distribution function* (NDF) $D(\mathbf{h})$. The NDF represents the most high-frequency characteristics of the surface reflectance. The shadowing term $S(\mathbf{k})$ approximates the shadowing and masking effects of microfacets [Bec65, Smi67, APS00] and can be derived from $D(\mathbf{h})$. Therefore, the four quantities we want to measure are: the NDF $D(\mathbf{h})$, the Fresnel term $F(\mathbf{o},\mathbf{i})$, and the diffuse and specular coefficients k_d and k_s.

As $D(\mathbf{h})$ is defined on the half-vector domain, one BRDF slice captured by the condenser only covers a partial region of the NDF. Therefore in theory, it is impractical to cover entire hemisphere of the NDF from only one fixed condenser. However, by taking advantage of the BRDF symmetry property, our apparatus is capable of sampling the full NDF domain with one fixed condenser.

3.2. Symmetry Property of BRDFs

The symmetry properties of BRDFs are explored by [HLHZ08] for estimating normal and tangent vectors. They validate the symmetry properties on a wide range of real-world BRDFs, and only rare exceptions were found. In this paper, we assume the BRDF symmetry across the surface normal:

$$\rho(\mathbf{i},\mathbf{o}) = \rho(\tau\mathbf{i},\tau\mathbf{o}), \quad \tau = \begin{bmatrix} -1 & 0 & 0 \\ 0 & -1 & 0 \\ 0 & 0 & 1 \end{bmatrix} \tag{3}$$

where the half-vector of $\tau\mathbf{i},\tau\mathbf{o}$ and that of $\mathbf{i},\mathbf{o}$ are mirror reflected to each other respect to $\mathbf{n}$. The symmetry slice of measured BRDF covers the symmetrical NDF regions so that we only need to measure part of the NDF domain and complete the remaining region via symmetry. Please reference Figure 2 (c)(d) to see how the symmetry property completes the NDF domain.

4. Device Setup

To capture material reflectance, the material sample is illuminated by a set of directional lights, and the reflected rays over a hemispherical field are gathered by a pair of condensers and captured by a fixed position CCD. From the captured data, high-resolution partial normal distribution functions (NDFs) are reconstructed and finally merged into a microfacet BRDF.

4.1. Optical Design

Figure 1 shows the design setup of our portable reflectometer. The core optical components are a pair of Anchor Optics $47mm$ condenser lenses with $21mm$ focal length. The condenser lenses concentrate light emitted from the sample surface at the focal point f_F into a projected beam, the beam passes through a $200\mu m$ pinhole f_O and captured by a Firefly MV camera from Point Gray Research. The light sources are 6 high-brightness LEDs; to generate a directional light beam the LED is attached to a carbon fiber tube.

In order to sample the NDF at a near grazing angle, both grazing angle lighting and viewing are required. We first place one LED light beam l_0 at 5 degrees above the horizontal plane, which is the nearest to grazing angle we can make due to the mechanical constraints. Then the optical axis of the condenser is set to the same azimuth angle, and the inclination as large as possible, in our case the inclination angle is 20 degree off the normal.

When the condenser is fixed, the partial NDF regions that can be captured are determined by the lighting setup. Figure 2(c) shows the partial NDF regions we captured with each light source. We manually determine the light source direction to maximize the coverage. The l_1 is placed at the grazing angle to cover NDF at high inclination angle; to maximize the inclination coverage, two light sources l_3 and l_6

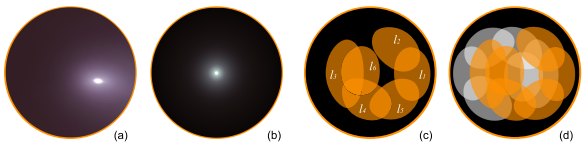

Figure 2: *(a) One measured BRDF slice. (b) Reconstructed NDF. (c) Partial NDF covered by each light source. (d) NDF completed by symmetry.*

are placed at a azimuthal symmetrical but different inclination angles. The last three light sources l_2, l_4 and l_5 connect the captured partial NDF together, and fill the remaining NDF regions. With those partial NDFs sampled, we can easily generate a full NDF via symmetry completion. In Figure 2, the NDF regions completed via symmetry are marked in gray, note how our samples covers the entire NDF domain. The sampled partial NDFs also overlap each other and the overlap regions provide sufficient information to accurately recover the Fresnel term.

When choosing the light directions, we also avoid adding LED light sources in the main light path between the two condensers, otherwise the shadow of the LED will introduce visible artifacts to the captured BRDFs.

4.2. Calibration

We assemble the reflectometry on a optical table, in a bottom up manner. We aimed a laser at a diffuse paper to simulate a point light source at f_F marked in Figure 1, and take it as the assembly base line. Then the first condenser lens is mounted, we adjust the lens so that lights from the point light source are concentrated into a parallel beam as designed. After that, the second condenser lens is added with, the base line light beam will focused on the focal point f_O. When setting the pinhole, it should not block any light go through the condenser lenses, otherwise it is not at the correct focal point. The camera and LED light sources are then added.

After the reflectometry is assembled, we calibrate the overall radiance transmission and optical distortion. The attenuations between light paths are different to each other, and the intensity variation of the LED light sources also need to be calibrated. We do the radiance calibration by measuring a Lambertian surface. We calculate a 2D scaler field for the captured image. The intensities of the LED lights are also calibrated by comparing BRDF slices captured from different LEDs

To calibrate the radial distortion, we put a occluder with pinhole grid between the base line point light source and the front condenser. With known relative position between the pinholes and the light source, the direction of rays that pass through the pinholes can be calculated. With multiple images captured with different occluder positions, we then perform a geometrical calibration as in [Zhang 2000] to correct the radial distortion of the condenser lenses.

When measuring the surface, the actual surface normal may have a slight deflection. We estimate such deflections in our data processing pipeline, as described in section 5.4.

4.3. Capturing Reflectance

As shown in Figure 1 the main component of the reflectometer is a cylinder 50mm in diameter and 120mm tall. The overall weight is less than 400g. We place the reflectometer over the material sample, the camera captures 2 images at different exposures for each LED light, and the image sets are then merged into an HDR image [DM97] in post processing. The Firefly camera is set in trigger mode, and controlled by a external circuit. The circuit also controls the LED lights, thus the light and camera are synchronized. The camera captures images with 320×240 resolution; the maximal exposure time is 8mm, and the BRDF capture rate is about 10 BRDFs per second.

5. BRDF Reconstruction

With the captured 6 BRDF slices, the microfacet BRDF is reconstructed in a iterative way. We first estimate the relative refraction index η for removing the Fresnel term. Then 6 partial NDFs are reconstructed and a shadowing term is derived. With the derived shadowing term, we can refine the relative refraction index estimation iteratively. After the iteration converges, we complete the NDF using the BRDF symmetry property.

The overall BRDF reconstruction process is described as follows:

BRDF Reconstruction
- *Estimate the Altered Normal*
- Repeat following steps until convergence
  - *Estimate the Fresnel Term*
  - Repeat following steps until convergence
    - *Reconstruct Partial NDF*
- *Complete the NDF*

5.1. Estimating the Fresnel Term

The Fresnel term $F(\mathbf{o},\mathbf{i})$ describes the specular reflectance near grazing angles. We followed [CT82] to model the Fresnel term:

$$F(\mathbf{o},\mathbf{i}) = \frac{(g-c)^2}{2(g+c)^2}\left(1+\frac{(c(g+c)-1)^2}{(c(g-c)+1)^2}\right), \qquad (4)$$

where $c = |\mathbf{o}\cdot\mathbf{h}|$, and $g^2 = \eta^2 + c^2 - 1$, η is the relative refraction index of the material.

If two measurement $\mathbf{i}_a,\mathbf{o}_a$ and $\mathbf{i}_b,\mathbf{o}_b$ have same half-angle, their $D(\mathbf{h})$ are same, thus the ratio between the two measured reflectances is determined by the Fresnel term and the shadowing term, and we can derive the ratio of Fresnel terms by:

$$\frac{F(\mathbf{i}_a,\mathbf{o}_a)}{F(\mathbf{i}_b,\mathbf{o}_b)} = \frac{\rho_s(\mathbf{i}_a,\mathbf{o}_a)S(\mathbf{i}_b)S(\mathbf{o}_b)(\mathbf{i}_a\cdot\mathbf{n})(\mathbf{o}_a\cdot\mathbf{n})}{\rho_s(\mathbf{i}_b,\mathbf{o}_b)S(\mathbf{i}_a)S(\mathbf{o}_a)(\mathbf{i}_b\cdot\mathbf{n})(\mathbf{o}_b\cdot\mathbf{n})} \qquad (5)$$

We first assume the shadowing term is constant $S(\mathbf{k}) = 1$, then the relative refraction index η is estimated by minimizing:

$$E(\eta) = \sum || \frac{F_m(\mathbf{i}_a, \mathbf{o}_a)}{F_m(\mathbf{i}_b, \mathbf{o}_b)} - \frac{F_c(\mathbf{i}_a, \mathbf{o}_a, \eta)}{F_c(\mathbf{i}_b, \mathbf{o}_b, \eta)} ||^2 \quad (6)$$

where $F_m(\mathbf{i}, \mathbf{o})$ is the measured Fresnel term, and $F_c(\mathbf{i}, \mathbf{o}, \eta)$ is computed from equation 4. We solve the optimal η by Levenberg-Marquardt algorithm [P*92]

In some rare cases, the Fresnel term estimation results a abnormally large $E(\eta)$, that is mainly caused by the error introduced by incorrect measurement operations such as shaking or moving the device rapidly. Our system will automatically detect such cases and ignore such data.

5.2. Reconstruct Partial NDF

Here we fit the measured specular reflectance into partial NDF. Following [NDM05, WZT*08], we started with a constant shadowing term $S(\mathbf{k}) = 1$, and the partial NDF can be computed by:

$$D(\mathbf{h}) = \frac{4\pi\rho_s(\mathbf{i}, \mathbf{o}_h)(\mathbf{i} \cdot \mathbf{n})(\mathbf{o}_h \cdot \mathbf{n})}{S(\mathbf{i})S(\mathbf{o}_h)F_c(\mathbf{i}, \mathbf{o}_h, \eta)} \quad (7)$$

where $\mathbf{o}_h$ is $\mathbf{i}$ mirror reflected with respect to $\mathbf{h}$, F_c is calculated Fresnel term from the estimated refraction index η.

Then the shadowing term $S(\mathbf{k})$ can be computed by the following equation [APS00]

$$S(\mathbf{k}) = \frac{\mathbf{k} \cdot \mathbf{n}}{\int_{\Omega_+(k) \cap \Omega_+(n)} (\mathbf{k} \cdot \mathbf{h}) D(\mathbf{h}) \mathrm{d}\omega_h} \quad (8)$$

where the integration domain is defined as $\Omega_+(\mathbf{k}) = \{\mathbf{h} | \mathbf{h} \cdot \mathbf{k}\}$.

As mentioned in [WZT*08], we also constrain the shadowing term $S(\mathbf{k})$ over azimuthal angles that $S(\mathbf{k}) = min_{\mathbf{k}'}\{S(\mathbf{k}') | \mathbf{k}' \cdot \mathbf{n} = \mathbf{k} \cdot \mathbf{n}\}$. Since we have 6 measured BRDF slices, each slice can be fitted to a partial NDF D_i and a accompanied shadowing term S_i. We then average the 6 shadowing term S_i into one S to update the NDF via equation7.

The NDF and the shadowing term are updated iteratively until convergence. When the partial NDF reconstruction converges, we update the relative refraction index η for the Fresnel, the microfacet term and the Fresnel term are estimated iteratively until convergence. In general, the NDF and shadowing term iteration converge within 6 iterations, and the Fresnel term iteration converge within 5 iterations.

5.3. Completing the NDF

To complete the NDF, we use equation 3 to reflect measured BRDF samples and calculate the corresponding partial NDF $D(\mathbf{h})$ with reconstructed Fresnel term and shadowing term by equation 7. We followed the weighted merging step in [WZT*08] to merge partial NDF D_i into the full NDF D_f.

$$D_f(\mathbf{h}) = \frac{\sum W_i(\mathbf{h}) D_i(\mathbf{h})}{\sum W_i(\mathbf{h})}, \quad W(\mathbf{h}) = [\mathbf{o}_h \cdot \mathbf{n}]_+^{\frac{1}{2}}, \quad (9)$$

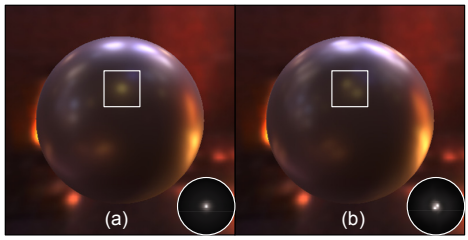

Figure 3: *Rendering results of reconstructed BRDF with normal estimation (a) and without normal estimation (b). The NDF of each result is presented at the bottom right. Note without normal estimation, the results will suffer the double image artifact caused by the altered specular peak.*

where $\mathbf{o}_h$ is $\mathbf{i}$ mirror reflected with respect to $\mathbf{h}$.

5.4. Estimating the Altered Normal

When positioning our apparatus by hand to measure a curved surface, it is hard to make sure the surface normal of the measured point is exactly upward as we require. To handle this, a normal estimation process is introduced before the microfacet BRDF reconstruction.

Our normal estimation is similar to [HLHZ08]. To estimate the actual normal, we find the $\mathbf{n}$ by minimizing the symmetry distance described in [HLHZ08]. Note we only use the symmetry distance with the reflection symmetry across the surface normal. Since we have dense view and sparse light measurements, the symmetry transformation is applied on $\mathbf{o}$ instead of $\mathbf{i}$. After the normal estimation, the lighting and viewing directions are then updated according to the estimated normal.

Figure 3 shows rendering results of reconstructed BRDFs with and without normal estimation. Without estimating the altered normal, the captured BRDF slices have an altered specular peak which causes the double image artifact.

5.5. Extension for Asymmetric BRDF

To handle rare cases when the BRDF symmetry property is not available, we follow [WZT*08], to complete the NDF by microfacet synthesis.

To measure an asymmetric NDF, instead of measuring once, we rotate the apparatus and capture multiple times on the same material sample. At each rotation position, a partial NDF at current local frame is reconstructed. Instead of using symmetry to mirror the partial NDF, we merge captured partial NDF with equation 9. We followed the synthesis criteria in [WZT*08] and perform a brute force search with those measured data to find the best match. The bottom left result in Figure 6 is rendered with a asymmetry BRDF that reconstructed via microfacet synthesis.

6. Experimental Results

To evaluate our method, we performed tests with the MERL BRDF dataset [MPBM03a], as well as the anisotropic BRDFs captured by [NDM05]. We also captured large variety of materials with our prototype device.

We implemented our microfacet reconstruction algorithm on a PC with Intel Xeon E5440 CPU and 4GB memory. The NDFs we reconstruct are stored in a hemicube with 512×512 pixels on top face and 512×256 pixels on each side. The reconstruction time for each BRDF is about 30 seconds.

6.1. Validation with Dense Measured BRDF

We evaluate our method with the MERL BRDF dataset [MPBM03a], which contains 100 isotropic BRDFs from near diffuse to highly specular materials. This data was captured by a gantry with moveable camera/lights that densely sampled the 4D full BRDF space. We select the light/view data pairs that would be sampled by our optical design as the input of our algorithm, and leave all other data as a validation reference. Figure 5 plots the reconstruction error of all the 100 BRDFs ordered by error.

The error is calculated by the error metric presented in [NDM05]

$$E(\mathbf{k}) = \sqrt{\frac{\sum w[R(\mathbf{i},\mathbf{o})(\mathbf{i}\cdot\mathbf{n}) - M(\mathbf{i},\mathbf{o})(\mathbf{i}\cdot\mathbf{n})]^2}{\sum w}} \qquad (10)$$

where w is the solid angle correction term, the errors are then normalized by the maximum albedo of each BRDF and plotted in logarithmic scale. Since Cook-Torrance typically have the lowest errors among the parametric models [NDM05], we choose this model to compare with. Figure 5 shows that our device always generates more accurate results than Cook-Torrance model. We also provided the rendering result comparisons for two typical cases, one for the largest error case and one that has significant visual improvement over parametric model. Note even in the largest error case, the reconstructed BRDF still captured enough details of the reflectance appearance.

6.2. Compare to Existing Reflectometry Apparatus

Existing reflectometry that perform full sampling over the 4D BRDF such as [Msy07] requires tens of minutes to capture a single BRDF. The only device that can achieve comparable measurement speed is the device described in [DWT*10].

Thus we compared the measured BRDF quality against the dense measured BRDF data set presented in [MPBM03a, NDM05]. The input data for the [DWT*10] apparatus is selected base on their optical design. The raw BRDF data captured by [NDM05] is not dense enough to provide required measurement data, so we fit the their data into a general microfacet model to generate required data. Note the reconstruction error is still measured against the raw BRDF data they actual measured.

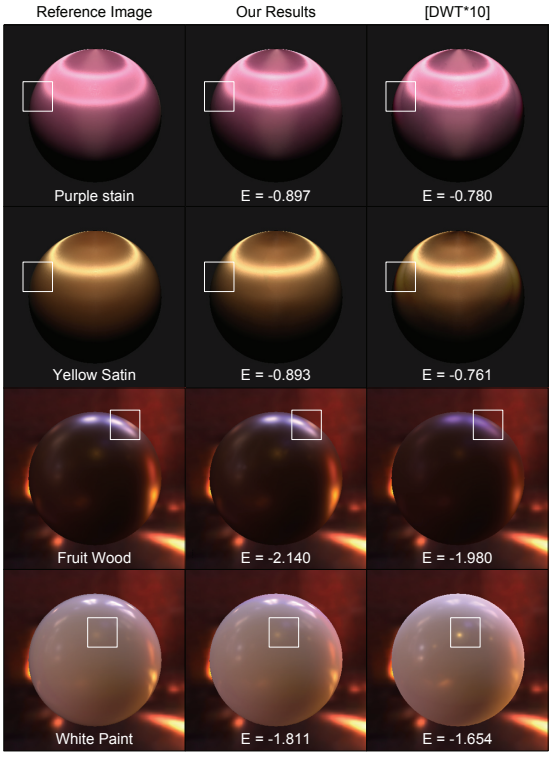

Figure 4: *Comparison of the rendering results of reconstructed BRDF with our apparatus and [DWT*10] to the reference rendered with full sampled BRDF. The purple stain and yellow stain are rendered with point light source to show the highly anisotropic appearance. The fruit wood and white paint are rendered with environment map lighting. Note how our method captures the reflectance details on the NDF as well as faithfully reproduces the Fresnel effects near the grazing angle.*

Figure 4 shows the rendered results as well as the numerical error comparison. Note how our apparatus captures the reflectance near grazing angles, and the rendered results match the reference images well. On the other hand, the apparatus proposed in [DWT*10] misses NDF features in the *purple stain* and *yellow satin* near the edge of the ball, and results in a visible artifact and large reconstruction error. The Fresnel effects in the *fruit wood* and *white paint* are well preserved by our approach. However, mismatched Fresnel factors result in a visibly incorrect high-light in [DWT*10]'s results.

6.3. Measured BRDF Data Set

With the portable instant reflectometer, we can easily measured a large variety of high quality BRDFs. Figure 6 shows the rendered results of 30 different BRDFs including 12

anisotropic BRDFs. The first three rows are isotropic BRDFs rendered with environment lighting, exhibiting appearance from near diffuse to highly specular. Note that the BRDFs shown in the first row exhibits different Fresnel effects at the edge of the ball. Several anisotropic BRDFs are captured and rendered with a teapot model shown in the last two rows. Notice how our method has well captured the anisotropic appearance of the material.

7. Conclusion

We present a practical and efficient solution for fast BRDF acquisition, especially for materials with anisotropic reflectance. The reflectometry apparatus we proposed is compact and portable which enables onsite measurements. We have tested the accuracy of our method by comparing our results with ground truth and demonstrate the efficiency of our reflectometry by a set of BRDFs with different specularity, Fresnel factors, and angular variations.

8. Acknowledgements

The authors would like to thank Moshe Ben-Ezra for helpful discussions about device building. We also thank the anonymous reviewers for their helpful suggestions and comments.

References

[APS00] ASHIKHMIN M., PREMOZE S., SHIRLEY P.: A microfacet-based BRDF generator. In *Siggraph 2000, Computer Graphics Proceedings* (2000), ACM Press / ACM SIGGRAPH / Addison Wesley Longman, pp. 65–74. 1, 2, 3, 5

[Bec65] BECKMANN P.: Shadowing of random rough surfaces. *IEEE Transactions on Antennas and Propagation*, 13 (1965), 384ÍC388. 3

[BEWB*08] BEN-EZRA M., WANG J., BENNETT W., LI X., MA L.: An LED-only BRDF measurement device. In *Computer Vision and Pattern Recognition, 2008. CVPR 2008. IEEE Conference on* (June 2008), pp. 1–8. 1, 2

[CT82] COOK R. L., TORRANCE K. E.: A reflectance model for computer graphics. *ACM Trans. Graph. 1*, 1 (1982), 7–24. 4

[Dan01] DANA K. J.: BRDF/BTF measurement device. In *Proceedings of eighth IEEE international conference on computer vision (ICCV)* (July 2001), vol. 2, pp. 460–466. 1, 2

[DHT*00] DEBEVEC P., HAWKINS T., TCHOU C., DUIKER H.-P., SAROKIN W., SAGAR M.: Acquiring the reflectance field of a human face. In *Proc. SIGGRAPH 2000* (2000), pp. 145–156. 2

[DM97] DEBEVEC P. E., MALIK J.: Recovering high dynamic range radiance maps from photographs. In *ACM SIGGRAPH* (1997), pp. 369–378. 4

[DNvGK99] DANA K. J., NAYAR S. K., VAN GINNEKEN B., KOENDERINK J. J.: Reflectance and texture of real-world surfaces. *ACM Transactions on Graphics 18*, 1 (1999), 1–34. 2

[DWT*10] DONG Y., WANG J., TONG X., SNYDER J., LAN Y., BEN-EZRA M., GUO B.: Manifold bootstrapping for svbrdf capture. vol. 31, ACM Press, pp. 762–771. 1, 2, 6

[GTHD03] GARDNER A., TCHOU C., HAWKINS T., DEBEVEC P.: Linear light source reflectometry. *ACM Trans. Graph. 22*, 3 (2003), 749–758. 1, 2

[GTLL06] GARG G., TALVALA E.-V., LEVOY M., LENSCH H. P. A.: Symmetric photography: exploiting data-sparseness in reflectance fields. In *Eurographics Workshop/ Symposium on Rendering* (Nicosia, Cyprus, 2006), Eurographics Association, pp. 251–262. 2

[GTR*06] GU J., TU C.-I., RAMAMOORTHI R., BELHUMEUR P., MATUSIK W., NAYAR S.: Time-varying surface appearance: acquisition, modeling and rendering. *ACM Trans. Graph. 25*, 3 (2006), 762–771. 2

[HLHZ08] HOLROYD M., LAWRENCE J., HUMPHREYS G., ZICKLER T.: A photometric approach for estimating normals and tangents. *ACM Transactions on Graphics 27*, 5 (2008), 1–9. 2, 3, 5

[HP03] HAN J. Y., PERLIN K.: Measuring bidirectional texture reflectance with a kaleidoscope. *ACM Trans. Graph. 22*, 3 (2003), 741–748. 1, 2

[KN06] KUTHIRUMMAL S., NAYAR S. K.: Multiview radial catadioptric imaging for scene capture. *ACM Trans. Graph. 25*, 3 (2006), 916–923. 2

[LBAD*06] LAWRENCE J., BEN-ARTZI A., DECORO C., MATUSIK W., PFISTER H., RAMAMOORTHI R., RUSINKIEWICZ S.: Inverse shade trees for non-parametric material representation and editing. *ACM Transactions on Graphics (Proc. SIGGRAPH) 25*, 3 (July 2006). 2

[LFTG97] LAFORTUNE E. P. F., FOO S.-C., TORRANCE K. E., GREENBERG D. P.: Non-linear approximation of reflectance functions. In *SIGGRAPH '97: Proceedings of the 24th annual conference on Computer graphics and interactive techniques* (New York, NY, USA, 1997), ACM Press/Addison-Wesley Publishing Co., pp. 117–126. 1, 2

[LKG*03] LENSCH H. P. A., KAUTZ J., GOESELE M., HEIDRICH W., SEIDEL H.-P.: Image-based reconstruction of spatial appearance and geometric detail. *ACM Transaction on Graphics 22*, 2 (Apr. 2003), 234–257. 1, 2

[LKK98] LU R., KOENDERINK J. J., KAPPERS A. M. L.: Optical properties bidirectional reflectance distribution functions of velvet. *Applied Optics 37*, 25 (Sept. 1998), 5974–5984. 1, 2

[LLSS03] LENSCH H. P. A., LANG J., SÁ A. M., SEIDEL H.-P.: Planned sampling of spatially varying BRDFs. *Computer Graphics Forum 22*, 3 (Sept. 2003), 473–482. 1, 2

[MLH02] MCALLISTER D. K., LASTRA A. A., HEIDRICH W.: Efficient rendering of spatial bi-directional reflectance distribution functions. In *Proceedings of the 17th Eurographics/SIGGRAPH workshop on graphics hardware (EGGH-02)* (New York, Sept. 1–2 2002), Spencer S. N., (Ed.), ACM Press, pp. 79–88. 2

[MMS*05] MULLER G., MESETH J., SATTLER M., SARLETTE R., KLEIN R.: Acquisition, synthesis, and rendering of bidirectional texture functions. *Computer Graphics Forum 24*, 1 (2005), 83–109. 2

[MPBM03a] MATUSIK W., PFISTER H., BRAND M., MCMILLAN L.: A data-driven reflectance model. *ACM Trans. Graph. 22*, 3 (2003), 759–769. 6

[MPBM03b] MATUSIK W., PFISTER H., BRAND M., MCMILLAN L.: Efficient isotropic BRDF measurement. In *EGRW '03: Proceedings of the 14th Eurographics workshop on Rendering* (Aire-la-Ville, Switzerland, Switzerland, 2003), Eurographics Association, pp. 241–247. 1, 2

[Msy07] MUKAIGAWA Y., SUMINO K., YAGI Y.: High-speed measurement of BRDF using an ellipsoidal mirror and a projector. In *Computer Vision and Pattern Recognition, 2007. CVPR '07. IEEE Conference on* (June 2007), pp. 1–8. 1, 2, 6

[MWL*99] MARSCHNER S., WESTIN S., LAFORTUNE E., TORRANCE K., GREENBERG D.: Image-based BRDF measurement

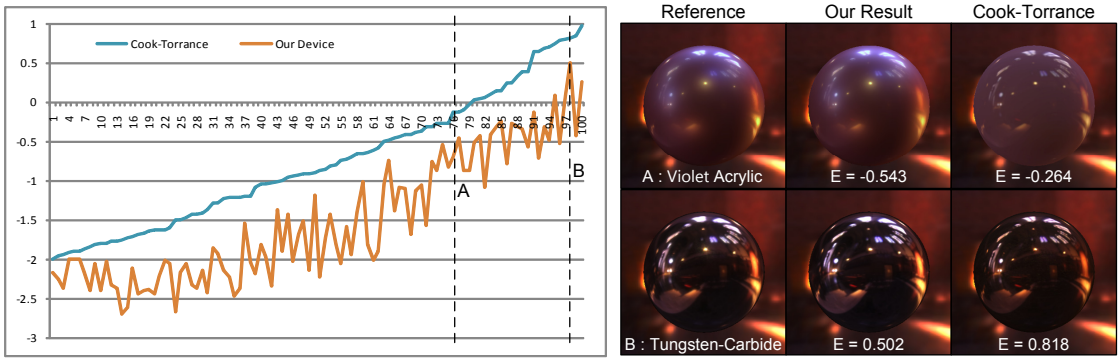

Figure 5: *The normalized reconstruction error of all the 100 MERL BRDFs. The BRDFs are sorted by the error of Cook-Torrance model for visualization purpose. The rendering results comparisons are also provided for two typical cases.*

Figure 6: *Rendered results of a measured BRDF data set. Our results cover BRDFs with different specularity, Fresnel factors and angular variations.*

including human skin. In *10th Eurographics Rendering Workshop* (1999). 1, 2

[NDM05] NGAN A., DURAND F., MATUSIK W.: Experimental analysis of BRDF models. *Eurographics Symposium on Rendering 2005* (2005). 1, 2, 5, 6

[NRH*77] NICODEMUS F. E., RICHMOND J. C., HSIA J. J., GINSBERG I. W., LIMPERIS T.: Geometric considerations and nomenclature for reflectance. *Monograph 161,National Bureau of Standards (US)* (1977). 1

[P*92] PRESS W. H., ET AL.: Numerical recipes in C (second edition). *Cambridge University Press* (1992). 5

[RVZ08] ROMEIRO F., VASILYEV Y., ZICKLER T.: Passive reflectometry. In *ECCV '08: Proceedings of the 10th European Conference on Computer Vision* (Berlin, Heidelberg, 2008), Springer-Verlag, pp. 859–872. 2

[Smi67] SMITH B. G.: Geometrical shadowing of a random rough surface. *IEEE Transactions on Antennas and Propagation*, 15 (1967), 668 – 671. 3

[War92] WARD G. J.: Measuring and modeling anisotropic reflection. In *SIGGRAPH '92: Proceedings of the 19th annual conference on Computer graphics and interactive techniques* (New York, NY, USA, 1992), ACM Press, pp. 265–272. 1, 2

[WZT*08] WANG J., ZHAO S., TONG X., SNYDER J., GUO B.: Modeling anisotropic surface reflectance with example-based microfacet synthesis. In *SIGGRAPH '08: ACM SIGGRAPH 2008 papers* (New York, NY, USA, 2008), ACM, pp. 1–9. 1, 2, 5